

Local myocardial insulin-like growth factor 1 (IGF-1) delivery with biotinylated peptide nanofibers improves cell therapy for myocardial infarction

Michael E. Davis*, Patrick C. H. Hsieh*, Tomosaburo Takahashi*, Qing Song[†], Shuguang Zhang[†], Roger D. Kamm[†], Alan J. Grodzinsky[†], Piero Anversa[‡], and Richard T. Lee*^{†§}

*Cardiovascular Division, Department of Medicine, Brigham and Women's Hospital, Harvard Medical School, Boston, MA 02139; [†]Division of Biological Engineering, Massachusetts Institute of Technology, Cambridge, MA 02139; and [‡]Cardiovascular Research Institute, Department of Medicine, New York Medical College, Valhalla, NY 10595

Communicated by Eugene Braunwald, Harvard Medical School, Boston, MA, April 11, 2006 (received for review October 14, 2005)

Strategies for cardiac repair include injection of cells, but these approaches have been hampered by poor cell engraftment, survival, and differentiation. To address these shortcomings for the purpose of improving cardiac function after injury, we designed self-assembling peptide nanofibers for prolonged delivery of insulin-like growth factor 1 (IGF-1), a cardiomyocyte growth and differentiation factor, to the myocardium, using a "biotin sandwich" approach. Biotinylated IGF-1 was complexed with tetravalent streptavidin and then bound to biotinylated self-assembling peptides. This biotin sandwich strategy allowed binding of IGF-1 but did not prevent self-assembly of the peptides into nanofibers within the myocardium. IGF-1 that was bound to peptide nanofibers activated Akt, decreased activation of caspase-3, and increased expression of cardiac troponin I in cardiomyocytes. After injection into rat myocardium, biotinylated nanofibers provided sustained IGF-1 delivery for 28 days, and targeted delivery of IGF-1 *in vivo* increased activation of Akt in the myocardium. When combined with transplanted cardiomyocytes, IGF-1 delivery by biotinylated nanofibers decreased caspase-3 cleavage by 28% and increased the myocyte cross-sectional area by 25% compared with cells embedded within nanofibers alone or with untethered IGF-1. Finally, cell therapy with IGF-1 delivery by biotinylated nanofibers improved systolic function after experimental myocardial infarction, demonstrating how engineering the local cellular microenvironment can improve cell therapy.

engineering | maturation | scaffold

Although there is great enthusiasm to repair the heart by using cell therapy, studies to date indicate that few transplanted cells engraft and ultimately function normally within the host tissue (1, 2). Investigators have attempted to improve cell therapy by a variety of strategies (3). Quantitative control of transplanted cell fate has been a shortcoming of many therapeutic strategies. Thus, targeted and controlled delivery of growth factors to the local environment could improve transplanted cell survival and function.

Substantial data suggest that insulin-like growth factor 1 (IGF-1) is a potent cardiomyocyte growth and survival factor. Mice deficient in IGF-1 have increased apoptosis after myocardial infarction (4), whereas cardiac-specific IGF-1 overexpression protects against myocyte apoptosis and ventricular dilation after infarction (5, 6). IGF-1 overexpression increases cardiac stem cell number and growth, leading to an increase in myocyte turnover and function in the aging heart (6). After infarction, IGF-1 promotes engraftment, differentiation, and functional improvement of embryonic stem cells transplanted into myocardium (7). However, IGF-1 is a small protein that diffuses readily through tissues, a property that allows it to signal over great distances (8), but this property could restrict its retention within a tissue for prolonged periods.

Self-assembling peptides are oligopeptides composed of alternating hydrophilic and hydrophobic amino acids (9, 10). On exposure to physiological osmolarity and pH, the peptides rapidly assemble into small nanofibers (≈ 10 nm) that can be injected into the myocardium to form 3D cellular microenvironments (11, 12). These peptide nanofiber microenvironments recruit a variety of cells including vascular cells (12). In this article, we describe development of a delivery system using a "biotin sandwich" approach that allows coupling of a factor to peptide nanofibers without interfering with self-assembly. Biotinylation of self-assembling peptides allowed specific and highly controlled delivery of IGF-1 (the Ea isoform; see ref. 13) to local myocardial microenvironments, leading to improved results of cell therapy. Although we describe controlled myocardial delivery here, this approach may be used to delivery one factor or even multiple factors to tissues for prolonged periods.

Results

Selective Binding to Self-Assembling Nanofibers Through Streptavidin-Biotin Linkages. We have shown that biotinylated peptides can be incorporated by self-assembly into nanofibers (14). To allow sufficient distance from the peptide to permit streptavidin binding (15, 16), the biotin was attached to the peptide by two *N*^ε-fluorenylmethoxycarbonyl- ϵ -aminocaproic acids. To determine the affinity for streptavidin binding to the biotinylated self-assembling peptides, we performed binding assays using ³⁵S-streptavidin and 1:100 biotinylated peptides/nonbiotinylated peptides (1% final peptide wt/vol). The apparent K_d was 1.9×10^{-7} M (Fig. 1A). Although this dissociation constant is substantially higher than the dissociation constant for unbound biotin and streptavidin in solution, this result is consistent with reports of polymer conjugation and biotin-streptavidin affinity (17, 18). To demonstrate streptavidin binding to the peptide nanofibers, we visualized the peptides with and without streptavidin using atomic force microscopy (AFM). As the AFM images in Fig. 1B show, streptavidin bound to the biotinylated nanofibers (arrows). The AFM images of streptavidin were consistent with published AFM images of streptavidin alone (19). These experiments show that streptavidin can be coupled to the biotinylated peptides in a specific manner.

Biotin Sandwich for Tethering of IGF-1 to the Peptide Fibers. We then developed a biotin sandwich method for targeting IGF-1 to the peptides, taking advantage of the four binding sites available on each streptavidin. Biotinylated IGF-1 and streptavidin were

Conflict of interest statement: No conflicts declared.

Abbreviations: IGF-1, insulin-like growth factor 1; AFM, atomic force microscopy; dnAkt, dominant negative Akt.

[§]To whom correspondence should be addressed at: Partners Research Facility, Room 280, 65 Landsdowne St., Cambridge, MA 02139. E-mail: rlee@rics.bwh.harvard.edu.

© 2006 by The National Academy of Sciences of the USA

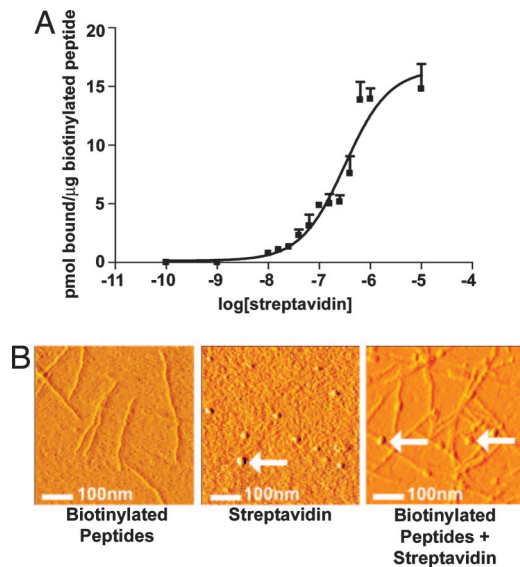


Fig. 1. Streptavidin-binding to the biotinylated peptides. (A) Binding curve demonstrating the binding capacity of ^{35}S -streptavidin to biotinylated self-assembling peptides. (B) AFM images of the biotinylated self-assembling peptide nanofibers alone (Left), streptavidin alone (Center), or streptavidin coupled to the biotinylated self-assembling peptide nanofibers (Right). Arrows show spherical streptavidin molecules.

mixed in a 1:1 molar ratio, allowing other biotin-binding sites on most tetravalent streptavidins to remain available for binding to the biotinylated self-assembling peptides (Fig. 2A). To test this method, we incubated biotinylated IGF-1 bound to streptavidin with either biotinylated or nonbiotinylated self-assembling peptides for 1 h. IGF-1 protein binding was increased 4.9 ± 0.4 -fold with biotinylated peptides compared with control nonbiotinylated peptides (Fig. 2B). Identical results were obtained when IGF-1 was mixed with the peptides during self-assembly or added after the self-assembly had occurred. These data confirmed that the biotin sandwich method for delivery of IGF-1 is feasible.

Biotinylated IGF-1 Is Active and Promotes Cell Survival and Maturation in 3D Culture. To verify that biotinylation of IGF-1 did not interfere with bioactivity, we treated rat neonatal cardiac myocytes with biotinylated IGF-1 or nonbiotinylated IGF-1 and examined Akt phosphorylation, a downstream target of IGF-1 signaling. Biotinylated IGF-1 induced Akt phosphorylation to the same degree as nonbiotinylated IGF-1 (Fig. 3A). These data suggest that specific

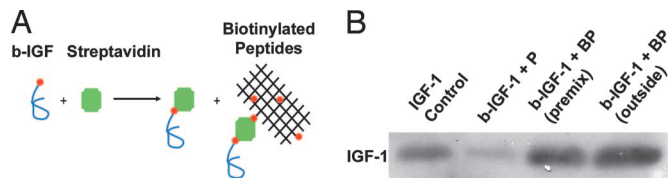


Fig. 2. Coupling to biotinylated self-assembling peptide nanofibers with the biotin sandwich approach. (A) Schematic showing the biotin sandwich method of tethering biotinylated IGF-1 (b-IGF-1) to biotinylated self-assembling peptides by using tetravalent streptavidin. This process does not interfere with self-assembly of peptides. (B) Representative Western blot analysis demonstrating tethering of biotinylated IGF-1 only to the biotinylated self-assembling peptides (b-IGF-1 + BP) and not the control nonbiotinylated peptides (b-IGF-1 + P). Premixing b-IGF-1 with biotinylated peptides vs. adding b-IGF-1 after self-assembly of biotinylated peptides occurred made no difference to b-IGF-1 binding.

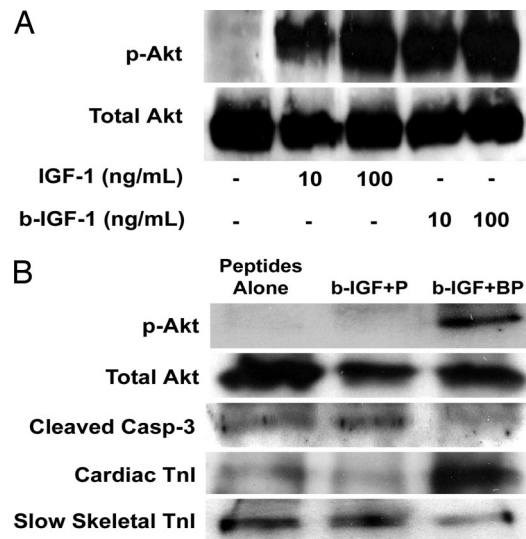


Fig. 3. Bioactivity of biotin sandwich and effect on cardiomyocytes. (A) Representative Western blot analysis demonstrating equivalent abilities of IGF-1 and biotinylated IGF-1 sandwich (b-IGF-1) to cause phosphorylation of Akt. (B) Representative Western blot analyses demonstrating increased activation of the survival factor Akt, decreased activation of caspase-3, and increased maturation markers [increased cardiac troponin I (TnI) and decreased slow skeletal troponin I] with tethered b-IGF-1 coupled with streptavidin in biotinylated peptides (b-IGF-1 + BP) compared with peptides alone and untethered b-IGF-1 coupled with streptavidin with control nonbiotinylated peptides (b-IGF-1 + P).

targeting of IGF-1 can be achieved with the biotinylated IGF-1 biotin sandwich method without interfering with bioactivity.

To test the biological effect of prolonged IGF-1 delivery, we cultured cardiac myocytes in self-assembling peptides alone, peptides with untethered IGF-1 (b-IGF-1 + streptavidin + nonbiotinylated peptides), and peptides with tethered IGF-1 (b-IGF-1 + streptavidin + biotinylated peptides) for 14 days. Phosphorylation of Akt was significantly increased (4.8 ± 0.8 -fold compared with control; $P < 0.01$) only in the tethered IGF-1 samples, with no changes in overall Akt levels (Fig. 3B). Furthermore, tethered IGF-1 significantly reduced cleavage of caspase-3, a marker of apoptosis ($44 \pm 5\%$ compared with control; $P < 0.01$). In addition, tethered IGF-1 changed expression of troponin I isoforms in a manner consistent with maturation. During maturation, there is a switch in troponin I isoforms in the heart from slow skeletal troponin I to cardiac troponin I (20). Tethering of IGF-1 significantly decreased slow skeletal troponin I ($63 \pm 4\%$ compared with control; $P < 0.01$) and significantly increased cardiac troponin I levels (4.9 ± 1.6 -fold compared with control; $P < 0.01$; Fig. 3B). These data demonstrate that IGF-1 tethered through the biotin sandwich method promotes long-term activation of survival pathways and increases the expression of cardiac maturation markers. Furthermore, to determine whether neonatal myocytes cultured for extended periods of time in nanofibers containing tethered IGF-1 demonstrate increased protein synthesis, [^3H]phenylalanine incorporation was measured after a 24-h incubation and normalized to total DNA content. Tethered IGF-1 significantly increased new protein synthesis after 14 days compared with untethered IGF-1 or peptides alone (Fig. 4).

Tethered IGF-1 Can Be Delivered *in Vivo* and Is Bioactive. Next, we sought to determine whether specific delivery of IGF-1 with self-assembling peptides can be achieved *in vivo* for extended periods of time. Twenty-five nanograms of free nonbiotinylated human IGF-1 (negative control), biotinylated human IGF-1 bound to streptavidin in nonbiotinylated peptides (untethered

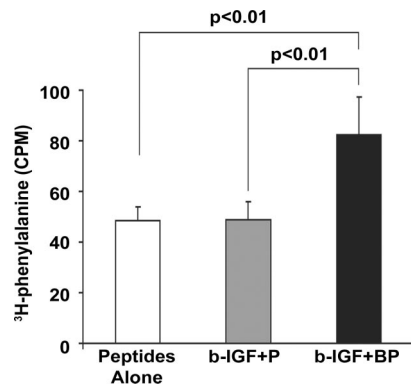


Fig. 4. Effect of tethered IGF-1 on new protein synthesis. Increase in cardiomyocyte [³H]phenylalanine incorporation after 14 days with tethered IGF-1 coupled with streptavidin in biotinylated peptide nanofibers (b-IGF-1 + BP) compared with peptide nanofibers alone and untethered IGF-1 coupled with streptavidin with control nonbiotinylated peptide nanofibers (b-IGF-1 + P).

IGF-1; negative control), or tethered IGF-1 with streptavidin coupled to biotinylated self-assembling peptides was injected into the myocardium of rats ($n \geq 4$ for each group per time point). Five minutes after injection, the human IGF-1 detected by species-specific ELISA was not different between groups. After 3 days, only 1.97 ± 1.18 ng of free IGF-1 remained, whereas 8.08 ± 0.60 ng of tethered IGF-1 bound to the biotinylated nanofibers far exceeded the negligible amounts in the control groups (Fig. 5A). This specific targeted delivery of IGF-1 was not observed with control peptides lacking biotin. After 3 months, however, there was a reduction in remaining IGF-1 in the tethered group with levels comparable to controls. To demonstrate *in vivo* biological activity of IGF-1 delivery, myocardial tissues 14 day after injection were stained for phospho-Akt. Activation of Akt was detected in tissues with tethered IGF-1 but not in control tissues without tethered IGF-1 (Fig. 5B).

Tethered IGF-1 Reduces Implanted Cardiomyocyte Apoptosis and Increases Cell Growth. To determine the effects of tethered IGF-1 on transplanted cells, isolated neonatal cardiac myocytes were labeled with the membrane dye PKHGL-2 and 50,000 cells were embedded within self-assembling peptides containing no IGF-1, untethered IGF-1, or tethered IGF-1. Tissues were harvested 14 days after myocardial injection ($n = 5$ animals per group, randomized and blinded). Tethered IGF-1 significantly reduced the percentage of implanted cells positive for cleaved caspase-3, an apoptosis marker ($31 \pm 2\%$ vs. $22 \pm 2\%$; $n \geq 160$ cells per group; $P < 0.01$, ANOVA followed by Dunnett's test; Fig. 6A). Additionally, in a separate randomized and blinded study of GFP-positive implanted cells, the cross-sectional area of cardiomyocytes injected with tethered IGF-1 was 25% greater than injected cells with no IGF-1 or untethered IGF-1 (16.3 ± 0.5 vs. $21.7 \pm 0.8 \mu\text{m}^2$; $n \geq 300$ cells per group; $P < 0.01$, ANOVA followed by Dunnett's test; Fig. 6B). These data demonstrate that IGF-1 can be delivered specifically to the myocardium with biotinylated self-assembling peptides and that this delivery activates critical survival pathways and improves transplanted cell growth.

Tethered IGF-1 Improves Cell Therapy After Experimental Myocardial Infarction. To determine whether tethered IGF-1 in the absence of cell therapy improves cardiac function after injury, we performed a blinded and randomized myocardial infarction study in 37 rats. IGF-1 alone, self-assembling peptides alone, and self-assembling peptides with or without tethered IGF-1 was injected into the

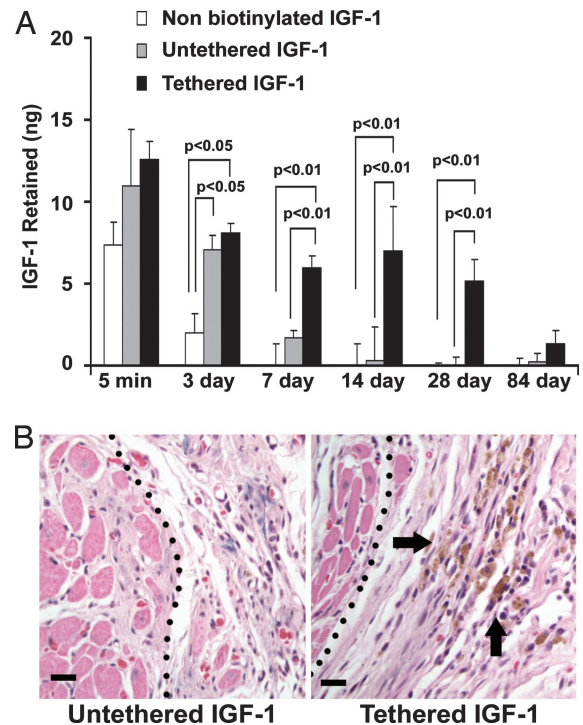


Fig. 5. *In vivo* delivery and bioactivity of tethered IGF-1. (A) Quantitative delivery of human IGF-1 to the myocardium of rats after 5 min and 7, 14, 28, and 84 days. Twenty-five nanograms of free nonbiotinylated IGF-1 (negative control), biotinylated IGF-1 bound to streptavidin in nonbiotinylated peptides (untethered b-IGF-1; negative control), or tethered b-IGF-1 with streptavidin coupled to biotinylated self-assembling peptides was injected into the myocardium of rats ($n \geq 4$ for each group per time point). (B) Immunohistochemistry showing phospho-Akt-specific staining in untethered b-IGF-1 (Left) and tethered b-IGF-1 (Right) samples. Arrows denote areas staining positive for phospho-Akt (brown staining). (Scale bars: 20 μm .)

infarct zone immediately after occlusion. An ECG 1 day and 21 days after infarction showed no differences in cardiac function (fractional shortening, wall thickness, and end diastolic diameter) among the treatment groups (data not shown). This null *in vivo* finding in the absence of cells was not surprising; we anticipated that isolated injected microenvironments with tethered IGF-1 in the absence of cells would have no beneficial effect on cardiac function.

In contrast, we hypothesized that inclusion of cells with IGF-1 would improve systolic function after infarction. We performed another randomized and blinded infarct study in 60 rats ($n \geq 7$ rats per group); 500,000 neonatal cardiomyocytes marked with a ade-

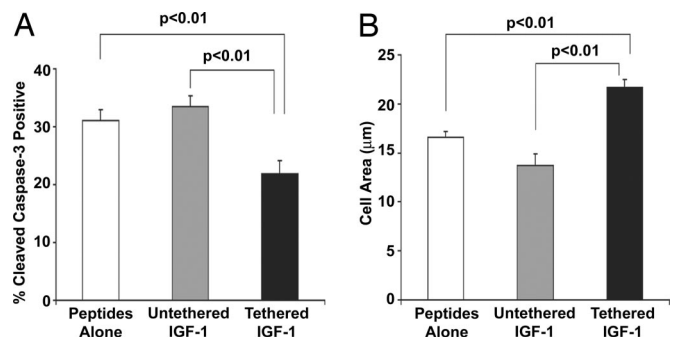


Fig. 6. Effects of tethered IGF-1 on survival and growth of implanted cells. Effects of tethered b-IGF-1 on implanted neonatal cardiac myocytes. Decreased cleavage of caspase-3 (A) and increased size (B) were found in cells embedded within tethered b-IGF-1 self-assembling peptides after myocardial implantation.

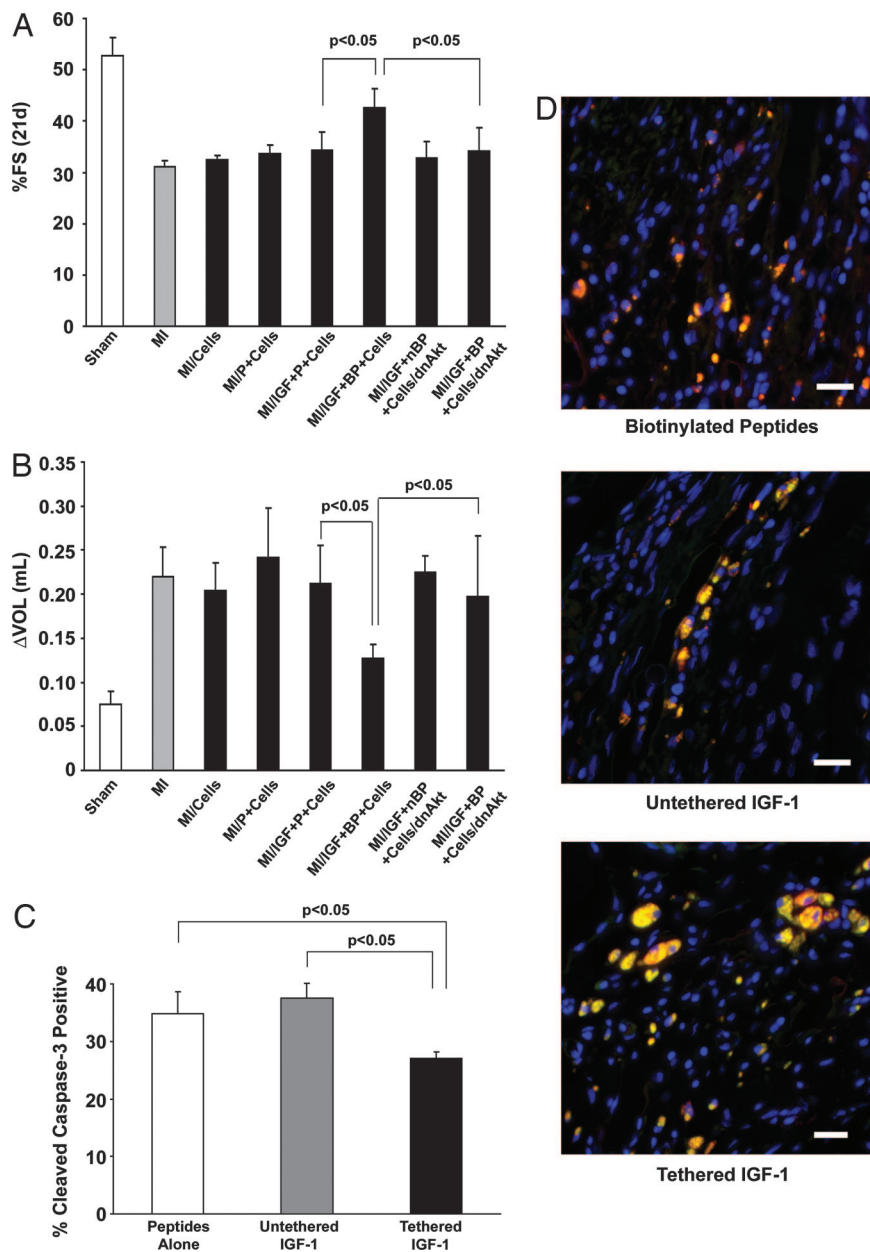


Fig. 7. Tethered IGF-1 improves efficacy of cell implantation on cardiac function after myocardial infarction. (A) Improvement in fractional shortening after 21 days in cells embedded within tethered b-IGF-1 containing self-assembling peptides (MI/IGF+BP) compared with untethered b-IGF containing self-assembling peptides (MI/IGF+P) and dominant negative transduced cells with tethered b-IGF-1 (MI/IGF+BP+Cells/dnAkt). (B) Ventricular dilation as measured by the increase in ventricular volume from 1 day to 21 days after infarction was not observed in rats treated with cells embedded within self-assembling peptides containing tethered b-IGF-1. (C) Cleavage of caspase-3 in implanted cells was significantly reduced in the presence of tethered IGF-1, whereas untethered IGF-1 had no effect. (D) Representative immunofluorescent staining showing cell size in treatment groups. GFP-positive cells (green) costained with tropomyosin (red) in peptides alone (*Top*), untethered (*Middle*), and tethered (*Bottom*) b-IGF-1 sections. Blue stain is DAPI (nuclei). (Scale bars: 20 μ m.)

novirus encoding GFP were injected alone, injected with self-assembling peptides, or injected with self-assembling peptides containing untethered or tethered IGF-1 after myocardial infarction. Additionally, cells infected with a hemagglutinin-tagged dominant negative Akt (dnAkt) adenovirus (21) were also injected with self-assembling peptides containing tethered IGF-1 and injected after myocardial infarction. GFP and dnAkt infection rates were 95–100%, and isolated neonatal myocytes infected with dnAkt had no phosphorylation of Akt in response to IGF-1 treatment, despite activation of the IGF-1 receptor (data not shown). There was no significant effect of any treatment at 1 day after infarction (data not shown). However, after 21 days, the tethered IGF-1 cell therapy

group had significantly improved fractional shortening compared with all other treatments (Fig. 7A). To determine whether targeted IGF-1 delivery attenuates ventricular dilation, a 2D analysis of ventricular volume (modified Simpson's method) was examined at 21 days after infarction and compared with levels from 1 day after infarction. Tethered IGF-1 attenuated ventricular dilation compared with untethered IGF-1, and this benefit was blocked by the dnAkt adenovirus (Fig. 7B). GFP-positive cells were also immunostained for cleaved caspase-3, and double-positive cells were counted. Similar to noninfarct studies, tethered IGF-1 delivery significantly reduced implanted myocyte apoptosis compared with delivery with peptides alone and untethered IGF-1 (Fig. 7C).

Immunofluorescent staining for tropomyosin colocalized with GFP demonstrated increased cell size in the tethered IGF-1 group (Fig. 7D). These data demonstrate that tethered IGF-1 improves the efficacy of cell therapy after infarction, preventing postinfarction ventricular systolic dysfunction as well as dilation.

Previous reports suggest that there may be an immune response to cell therapy in Sprague–Dawley rats due to differing major histocompatibility loci of this outbred strain (22). To examine this phenomenon, we performed a randomized and blinded study in 17 NIH nude rats, thus negating the host–graft response. In these animals, tethered IGF-1 still had a significant improvement over untethered IGF-1 when combined with cell therapy (21-day fractional shortening of $45 \pm 2\%$ vs. $36 \pm 3\%$; $P = 0.02$), suggesting a benefit of IGF-1 delivery independent of the immune response.

Discussion

In attempting cardiac repair with cell therapy, the fate of transplanted cells is a critical factor. Few injected cells survive injection into the myocardium (23), and it remains unclear if paracrine effects of injected cells, transdifferentiation, and/or recruitment of endogenous stem cells is responsible for apparent improvement in cardiac function in experimental studies (23). To date, the benefits of cell therapy remain unproven in humans because the majority of human studies have thus far been designed to demonstrate feasibility.

It is possible that death of transplanted cells may be one method by which transplanted cells may benefit the heart, perhaps by inducing an angiogenic response (23). However, it is logical that controlling cell fate after injection could provide an advantage for cell therapy. In this study, we demonstrate that self-assembling peptide nanofibers can provide specific and prolonged local myocardial delivery of a survival factor, IGF-1, using tetravalent streptavidin and biotinylated self-assembling peptides. Local delivery of IGF-1 increased cardiomyocyte growth both *in vitro* and *in vivo*, and this effect was consistent with an improvement in cell therapy efficacy after experimental infarction.

We designed the biotin sandwich method to deliver IGF-1 with biotinylated peptides to maximize the probability of peptide self-assembly and thus retention in the myocardium. Streptavidin and biotin-IGF-1 were combined in equimolar ratios and added to the biotinylated peptides. Because streptavidin contains 4 biotin-binding sites, the majority of biotin-IGF-1–streptavidin complexes have additional unoccupied sites to bind to the biotin moiety on the peptides. For this strategy, it was critical to show that the biotinylation of IGF-1 did not compromise bioactivity. Tethered IGF-1 remained capable of induction of phosphorylation of Akt, a downstream mediator of IGF-1 signaling, in cardiomyocytes. In addition, tethered IGF-1 peptides promoted cardiomyocyte maturation, as measured by a switch in cardiac troponin I isoforms and increased protein synthesis.

One possible approach to tethering factors to self-assembling peptides is to engineer fusion proteins with growth factors directly linked to the self-assembling peptide motifs. This approach would obviate the need for biotin–streptavidin complexes because the protein could be covalently linked to the peptide. However, it is possible that entropy or steric effects could limit fibril growth (24) and by implication, incorporation of fusion proteins into self-assembling peptide fibrils. In addition, the biotin sandwich approach can be considered a modular building-block strategy that could be used to multifunctionalize an injectable microenvironment. For example, building intramyocardial environments with different proteins in varying concentrations should be easily achieved.

Using a human-specific IGF-1 assay, we were able to quantify IGF-1 delivery *in vivo*. We found that free IGF-1 was rapidly eliminated from the myocardium, presumably through convective loss through capillaries or lymphatics. Embedding the IGF-1 in nonbiotinylated peptides (untethered IGF-1) increased IGF-1 retention at early time points, consistent with some nonspecific

binding to the peptide fibers, but only tethered IGF-1 was delivered at later time points. Additionally, the tethered IGF-1 was still active *in vivo*, resulting in detectable levels of phospho-Akt after 14 days. Tethered IGF-1 in the absence of cells did not protect cardiac function after myocardial infarction. We speculate that tethered IGF-1 is unable to diffuse out of the peptide microenvironment and protect nearby myocytes. Supporting this hypothesis is our finding that phosphorylation of Akt was detectable only within the peptide microenvironment and not in surrounding myocardium. Additionally, we did not examine the release mechanism of the tethered IGF-1. We speculate that the cells secrete proteases that degrade the peptides, allowing for local release of IGF-1.

The effects of tethered IGF-1 on implanted cells resulted in improved systolic function after infarction. Tethered IGF-1 combined with cell therapy not only improved fractional shortening but reduced ventricular dilation as well. Activation of Akt was critical to this recovery because cells infected with a dnAkt adenovirus did not restore function, even in the presence of tethered IGF-1. It is important to note, however, that the number of cells we transplanted (500,000) was probably less than the millions of cardiomyocytes lost in a typical myocardial infarction in the rat. Thus, it is unlikely that improved systolic function with tethered IGF-1 was due to a direct contribution of transplanted cells to contractile function. Future studies should define the secondary mechanisms by which relatively small numbers of cells may improve systolic function. Additionally, there was very little detectable cleaved caspase-3 in the native myocardium after 3 weeks, although we cannot exclude reduction of apoptosis in surrounding myocardium at an earlier time as a mechanism for the beneficial effects observed.

There are many challenges to the important goal of cardiac repair. In this article, we describe one approach that allows greater control of the intramyocardial environment by delivering growth factors to injured myocardium. With this system, it may be possible to design the local microenvironment to improve the endogenous regenerative response, for example, by delivery of a chemoattractant to promote stem cell migration. Although much more must be learned about why mammals have inadequate cardiac regeneration, the ability to control the local myocardial microenvironment may prove critical to preventing heart failure.

Materials and Methods

Self-Assembling Peptides. The RAD16-II peptide (AcN-RARA-DADARADADA-CNH₂) was synthesized by Synpep (Dublin, CA). Biotinylated RAD16-II peptide was synthesized at the Massachusetts Institute of Technology by adding a biotin molecule linked to the peptide by 2 *N*^ε-fluorenylmethoxycarbonyl- ϵ -aminocaproic acid groups. Immediately before injection, to initiate self-assembly, peptides were dissolved in sterile sucrose (295 mM) at 1% (wt/vol) and sonicated for 10 min. For all biotinylated peptide experiments, biotinylated and nonbiotinylated peptides were mixed in a 1:100 ratio before sonication.

AFM. Aliquots of 10 μ l were removed from the peptide solution at various times after preparation and deposited on a freshly cleaved mica surface. To optimize the amount of peptide adsorbed, each aliquot was left on mica for up to 2 min and then rinsed with 50–100 μ l of deionized water. Images were obtained by scanning the mica surface in air by an atomic force microscope (Multimode; Digital Instruments, Santa Barbara, CA) operating in tapping mode. Soft silicon cantilevers were chosen with a spring constant of 1–5 N/m and a tip radius of curvature of 5–10 nm. Typical scanning parameters were as follows: tapping frequency, ≈ 70 kHz; RMS amplitude before engage, 1–1.2 V; integral and proportional gains, 0.5–0.7 and 0.8–1.0, respectively; setpoint, 0.8–1 V; scanning speed, 0.5–2 Hz.

Human IGF-1 ELISA. Left ventricular free walls were excised 5 min or 3, 7, 14, 28, or 84 days after peptide injection and snap frozen in liquid nitrogen as described in ref. 25. The samples were then homogenized in a buffer containing Tris–Triton X-100 and analyzed for human-specific IGF-1 content with a human-specific IGF-1 ELISA (Diagnostic Systems Laboratories, Webster, TX).

Myocardial Infarction and Injection. Adult, male Sprague–Dawley rats weighing 250 g were obtained from Charles River Laboratories. The animals were anesthetized (60 mg/kg sodium pentobarbital), and after tracheal intubation, the hearts were exposed. Myocardial infarction was performed as described in ref. 25. Immediately after exposure of the heart (noninfarct studies) or coronary artery ligation, cells alone or embedded within the self-assembling peptides (80 μ l) were injected into the infarct zone through a 30-gauge needle, whereas the heart was beating. After injection, the chests were closed and animals were allowed to recover under a heating lamp. ECGs were performed 1 and 21 days after surgery. The animal protocols were approved by the Harvard Medical School Standing Committee on Animals.

Neonatal Cardiomyocyte Isolation. Cardiomyocytes from 1-day-old Sprague–Dawley pups (Charles River Laboratories) were obtained as described in ref. 12. The resulting cell pellet was resuspended in sucrose or self-assembling peptides for *in vitro* and *in vivo* studies. For *in vivo* infarction studies, the cells were incubated in suspension with an adenovirus (a multiplicity of infection of 150) for green fluorescent protein (GFP) or dnAkt (21) [a generous gift of K. Walsh (Boston University, Boston)] before embedding within the peptides.

Cell Culture Experiments. Neonatal cardiac myocytes were isolated, and 10^6 cells were suspended in 1% self-assembling

peptides alone, with 10 ng/ml untethered, or tethered IGF-1. After assembly, cells were cultured in serum-free medium (DMEM; Invitrogen) for 14 days. 3D cultures were homogenized by using TRI Reagent (Sigma), and protein was extracted according to manufacturer's protocol for Western analysis and [3 H]phenylalanine incorporation.

For adenovirus studies, cardiomyocytes were isolated and suspended in virus-containing serum-free medium for 2 h. Cells were either collected for flow cytometry analysis or plated on fibronectin-coated dishes and allowed to adhere for 24 h. Biotin-IGF-1 was then added for 15 min, and cells were harvested in $5\times$ sample buffer for Western analysis.

Materials. Radiolabeled Streptavidin ([35 S]sulfur-labeling reagent) and [3 H]phenylalanine were obtained from Amersham Pharmacia Biosciences. Purified human IGF-1 and anti-human IGF-1 antibody, as well as the green membrane dye PKHGL-2, were obtained from Sigma. Purified Streptavidin was obtained from Pierce. Biotinylated IGF-1 was obtained from Immunological and Biochemical Testsystems (Reutlingen, Germany) and used at a final concentration of 10 ng/ml in all experiments. Antibodies to total and phospho-Akt, phospho-IGF-1 receptor, and cleaved caspase-3 were obtained from Cell Signaling Technology. Antibody to cardiac troponin I was obtained from Chemicon. Antibody to slow skeletal Troponin I was obtained from Santa Cruz Biotechnology. Cy3-conjugated hemagglutinin antibody was obtained from Sigma.

Image Quantification. Densitometric analysis was performed by using SCION IMAGE (Scion, Frederick, MD).

This work was supported by National Institutes of Health Grants R01 HL081404, R01 EB003805, and F32 HL073574 and a grant from the Center for the Integration of Medicine and Innovative Technology.

- Menasche, P. (2003) *Ann. Thorac. Surg.* **75**, S20–S28.
- Menasche, P. (2004) *Curr. Opin. Cardiol.* **19**, 154–161.
- Mangi, A. A., Noiseux, N., Kong, D., He, H., Rezvani, M., Ingwall, J. S. & Dzau, V. J. (2003) *Nat. Med.* **9**, 1195–1201.
- Palmen, M., Daemen, M. J., Bronsaeer, R., Dassen, W. R., Zandbergen, H. R., Kockx, M., Smits, J. F., van der Zee, R. & Doevendans, P. A. (2001) *Cardiovasc. Res.* **50**, 516–524.
- Li, Q., Li, B., Wang, X., Leri, A., Jana, K. P., Liu, Y., Kajstura, J., Baserga, R. & Anversa, P. (1997) *J. Clin. Invest.* **100**, 1991–1999.
- Torella, D., Rota, M., Nurzynska, D., Musso, E., Monsen, A., Shiraiishi, I., Zias, E., Walsh, K., Rosenzweig, A., Sussman, M. A., et al. (2004) *Circ. Res.* **94**, 514–524.
- Kofidis, T., de Bruin, J. L., Yamane, T., Balsam, L. B., Lebl, D. R., Swijnenburg, R. J., Tanaka, M., Weissman, I. L. & Robbins, R. C. (2004) *Stem Cells* **22**, 1239–1245.
- Fraidenraich, D., Stillwell, E., Romero, E., Wilkes, D., Manova, K., Basson, C. T. & Benezra, R. (2004) *Science* **306**, 247–252.
- Zhang, S. (2003) *Nat. Biotechnol.* **21**, 1171–1178.
- Zhang, S., Holmes, T., Lockshin, C. & Rich, A. (1993) *Proc. Natl. Acad. Sci. USA* **90**, 3334–3338.
- Zhang, S., Marini, D. M., Hwang, W. & Santoso, S. (2002) *Curr. Opin. Chem. Biol.* **6**, 865–871.
- Davis, M. E., Motion, J. P., Narmoneva, D. A., Takahashi, T., Hakuno, D., Kamm, R. D., Zhang, S. & Lee, R. T. (2005) *Circulation* **111**, 442–450.
- Hameed, M., Orrell, R. W., Cobbold, M., Goldspink, G. & Harridge, S. D. (2003) *J. Physiol.* **547**, 247–254.
- Davis, M. E., Hsieh, P. C., Grodzinsky, A. J. & Lee, R. T. (2005) *Circ. Res.* **97**, 8–15.
- Livnah, O., Bayer, E. A., Wilchek, M. & Sussman, J. L. (1993) *Proc. Natl. Acad. Sci. USA* **90**, 5076–5080.
- Pugliese, L., Coda, A., Malcovati, M. & Bolognesi, M. (1993) *J. Mol. Biol.* **231**, 698–710.
- Stayton, P. S., Shimoboji, T., Long, C., Chilkoti, A., Chen, G., Harris, J. M. & Hoffman, A. S. (1995) *Nature* **378**, 472–474.
- Chan, B. P., Chilkoti, A., Reichert, W. M. & Truskey, G. A. (2003) *Biomaterials* **24**, 559–570.
- Neish, C. S., Martin, I. L., Henderson, R. M. & Edwardson, J. M. (2002) *Br. J. Pharmacol.* **135**, 1943–1950.
- Gao, L., Kennedy, J. M. & Solaro, R. J. (1995) *J. Mol. Cell. Cardiol.* **27**, 541–550.
- Fujio, Y. & Walsh, K. (1999) *J. Biol. Chem.* **274**, 16349–16354.
- Li, R. K., Mickle, D. A., Weisel, R. D., Mohabeer, M. K., Zhang, J., Rao, V., Li, G., Merante, F. & Jia, Z. Q. (1997) *Circulation* **96**, 179–186; discussion 186–187.
- Laflamme, M. A. & Murry, C. E. (2005) *Nat. Biotechnol.* **23**, 845–856.
- Caplan, M. R., Schwartzfarb, E. M., Zhang, S., Kamm, R. D. & Lauffenburger, D. A. (2002) *Biomaterials* **23**, 219–227.
- Hsieh, P. C., Davis, M. E., Gannon, J., MacGillivray, C. & Lee, R. T. (2006) *J. Clin. Invest.* **116**, 237–248.